Nematic-isotropic interface of some members of the homologous series of 4-cyano-4'-(*n*-alkyl)biphenyl liquid crystals

Sandro Faetti* and Vincenzo Palleschi
Dipartimento di Fisica dell' Università degli Studi di Pisa, Piazza Torricelli 2, I-56100 Pisa, Italy
(Received 17 April 1984)

The properties of the nematic-isotropic interface of some members of the homologous series of 4-cyano-4'-(*n*-alkyl)biphenyl liquid crystals [*n*-pentyl (5CB), *n*-hexyl (6CB), *n*-heptyl (7CB), and *n*-octyl (8CB)] are studied by optical reflectometry. The thickness of the interface is obtained by measuring the ratio of the actual reflected intensity to the value expected for a sharp interface. We find an effective thickness of order 400 Å in 5CB, 7CB, and 8CB, and of order 750 Å in 6CB. As shown by some authors, the effective thickness L is related to the superposition of two different contributions: an intrinsic diffuse profile due to density and order-parameter variations across the interface and an apparent diffuse profile of the interface due to surface capillary waves. Both of these contributions are accounted by us in our theoretical analysis. The intrinsic thickness is obtained in a satisfactory agreement with the predictions of the Landau—de Gennes theory. The easy polar angle is obtained by measuring the intensity anisotropy for the reflected extraordinary and ordinary waves. In all these samples the director is found to be tilted with respect to the vertical axis with a tilt angle which ranges from 48.5° in 8CB to 64.5° in 6CB. The anchoring energy coefficient W at the interface is obtained by applying an orienting torque by means of a horizontal magnetic field and by measuring the corresponding variation of the surface polar angle. We find W ranges from 0.84×10^{-4} erg/cm^2 rad^2 in 6CB to 8.5×10^{-4} erg/cm^2 rad^2 in 8CB. The experimental results are discussed in terms of the Landau—de Gennes expansion of the free energy and of the Parsons theory of the surface tension. All the phenomenological coefficients of this latter theory are obtained for the first time.

I. INTRODUCTION

In recent years there has been a growing interest in the physical properties of the interface between a liquid crystal (LC) and a different isotropic medium. In particular, many experiments have been performed to study the easy orientation of the average molecular axis (director $\vec{n}$) at the interface and its correlation with the physical and chemical properties of the interface. However, a full understanding of the physical mechanism responsible for the easy orientation of the director at these interfaces has not yet been reached. A review of most of the experimental and theoretical works in this field has been recently given by Cognard.[1]

The problem can be greatly simplified if one considers the case of the interface between a nematic LC and its vapor (free surface) or its isotropic phase (nematic-isotropic interface). In the last few years many phenomenological[2–7] or molecular theories[8–11] have been proposed that allow one to explain the main features of these interfaces. However, some important problems have not yet reached a full comprehension. In particular, most of the proposed theories cannot explain the tilt of the director which has been experimentally observed at the free surfaces of 4-methoxybenzilidene-4'-(*n*-butyl)aniline (MBBA) (Refs. 12—14) and 4-(*n*-ethoxy)benzilidene-4'-(*n*-butyl)aniline (EBBA) (Ref. 14) and at the nematic-isotropic interface of MBBA (Refs. 15—17) and of 7CB (Ref. 18). So far only the Parsons[4] and Mada[3] phenomenological theories seem to be able to explain these experimental observations. However, we point out that some aspects of the Mada theory have been recently criticized.[19]

The easy orientation of the director at the interface is due to the fact that the surface tension γ is a function of the polar angle θ which the director makes with the vertical z axis orthogonal to the interface. In the absence of external torques the symmetry of the interface requires γ to be independent of the azimuthal angle in the horizontal plane. Figure 1 shows schematically two possible

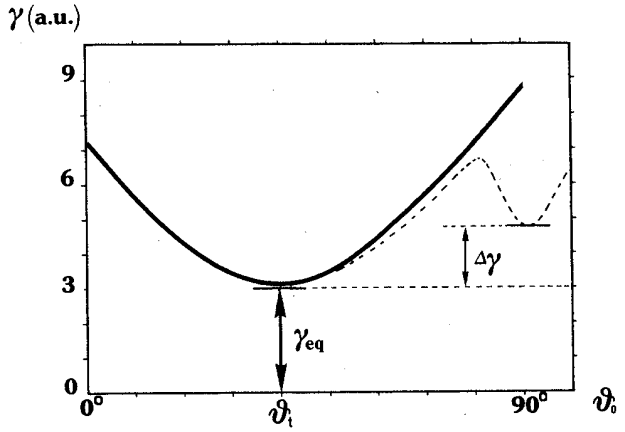

FIG. 1. Surface excess of free energy vs the polar angle θ_0 between the director and the axis orthogonal to the interface. Two possible dependences on θ_0 are represented by the solid and dashed curves, respectively. θ_t and γ_{eq} are the easy polar angle and the equilibrium surface tension, respectively.

 ©1984 The American Physical Society

behaviors of the surface tension $\gamma(\theta)$. At the equilibrium, the director polar angle assumes the easy value θ_t (tilt angle) which minimizes the surface tension. Close to $\theta=\theta_t$ the surface tension can be approximated by the simple relation

$$\gamma=\gamma_{eq}+W(\theta-\theta_t)^2+\cdots , \quad (1)$$

where the ellipsis represents unspecified higher-order terms, W represents the "anchoring energy coefficient" and γ_{eq} is the surface tension at the equilibrium position $\theta=\theta_t$. W gives a direct measure of the restoring torque which tends to align the director along the easy axis.

Another important parameter which characterizes the interface is represented by its thickness. As pointed out by some authors[20] in the case of the interface between an isotropic fluid and its vapor, the optically measured value of the thickness L (effective thickness) of the interface is related to two concomitant contributions:

(1) the intrinsic diffuse profile due to variations of the fluid density across the interface (intrinsic thickness L_0) and

(2) the apparent diffuse profile due to thermal fluctuations of the interface (apparent thickness L_T).

These contributions are schematically shown in Fig. 2. In the case of the interface between the nematic and isotropic phases both these contributions are expected to be relevant. The intrinsic thickness L_0 is mostly due to order-parameter variations across the interface. According to the Landau–de Gennes theory of the nematic-isotropic interface,[21] L_0 should be related to the anisotropic coherence length ξ ($L_0=4\xi$) of fluctuations of the scalar order parameter S at the clearing temperature T_c. This coherence length is expected to increase greatly as the temperature approaches the clearing temperature according to the functional dependence

$$\xi(T)=\xi_0\left[\frac{T^*}{T-T^*}\right]^{1/2} ,$$

where ξ_0 is a characteristic length of the order of the molecular length (~ 10 Å) and T^* is a critical temperature close to the clearing value T_c ($T_c-T^*\sim 1$ °C). The coherence length $\xi(T)$ can be measured by light scattering experiments. In the case of the nematic LC MBBA Gulari and Chu[22] found $\xi(T_c)=115\pm 15$ Å.

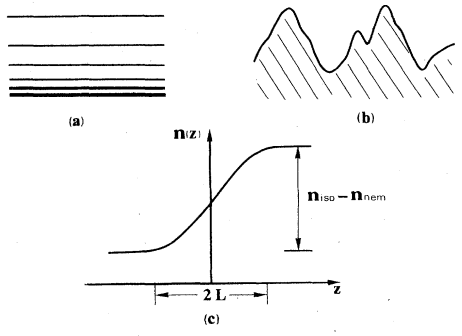

FIG. 2. Schematic view of the two physical effects which give a reduction of the intensity of the reflected light: (a) intrinsic diffuse profile of the interface; (b) apparent diffuse profile due to fluctuations; and (c) resulting variation of the average refractive index vs the z vertical coordinate.

As concerns the apparent thickness L_T due to thermal fluctuations, we notice also that this contribution can be relevant. In fact, strong thermal fluctuations of the interface are expected because of the very small value of the surface tension[23] and of the very small density difference between the two phases.[24]

From the previous discussion it is evident that a detailed understanding of the interfacial properties requires that all the parameters γ_{eq}, θ_t, W, and L_0 are known. Unfortunately so far few experimental data on the structural properties of the free surface and of the nematic-isotropic interface have been reported. In particular, for what concerns the nematic-isotropic interface, the director orientation at the interface has been measured only in MBBA (Refs. 15–17) and in 7CB (Ref. 18), while the anchoring energy has been measured only in 7CB (Ref. 18).

In a previous letter,[18] we reported experimental measurements of θ_t, L, and W at the nematic-isotropic interface of the nematic LC n-heptyl-4′-cyanobiphenyl (7CB). In this paper we extend these measurements to other members of the same homologous series (5CB, 6CB, and 8CB). All these samples exhibit a very high chemical stability and purity that allows us to obtain a good reproducibility of the experimental data. Chemical stability and purity are, indeed, very important to study surface properties of LC since these are noticeably affected by impurities.[12,16] The easy polar angle θ_t of the director, the anchoring energy coefficient W, and the interfacial thickness are measured for all these nematic compounds. θ_t is found to lie in the range from 50° to 70° while the anchoring energy coefficient W ranges from a minimum value of 8.4×10^{-5} erg/cm^2 rad^2 in 6CB to a maximum value of 8.5×10^{-4} erg/cm^2 rad^2 in 8CB. The measurements of θ_t and W are discussed in terms of the phenomenological Parsons theory[4] and allows us to obtain the first experimental values of the three phenomenological coefficients of this theory (γ_0, γ_P, and γ_Q).

The effective thickness L of the nematic-isotropic interface is found to be of the order of 400 Å in 5CB, 7CB, and 8CB and of the order of 750 Å in 6CB. These experimental results are discussed in terms of the two already described contributions (diffuse profile, thermal fluctuations). By using the experimental values of the surface tension γ_{eq} (Ref. 23) we are able to obtain a higher limit to the intrinsic thickness L_0 and, in turn, to the bulk coherence length ξ which is related to L_0 by (21):

$$\xi=\frac{L_0}{4} .$$

These latter experimental results are discussed in terms of the Landau–de Gennes theory of the interface.

II. EXPERIMENTAL PROCEDURES

A. Reflectivity coefficients in a stratified medium

The principle underlying our measurements has been already described by Bouchiat and Langevin[12] and by

Chiarelli *et al.*;[14] therefore, we here summarize only the main ideas. In the absence of external fields the director at the nematic-isotropic interface forms a well-defined polar angle θ_t with the vertical axis, while all the values of the azimuthal angle ϕ are equally probable. In order to measure θ_t, the director must be oriented along an x axis in the horizontal plane. This condition is accomplished by applying a horizontal magnetic field along the x axis which forces the director to orient itself with only two possible azimuthal angles ($\phi=0°$ and 180°). In this case, the polar angle of the director in the bulk is a function of the z coordinate that ranges from the surface value $\theta_0=\theta(H)$ to the bulk value $\theta(-\infty)=90°$. The thickness of the distorted layer is of the order of a few magnetic coherence lengths ξ_H.[14] If the nematic-isotropic interface is not sharp, but has a diffuse profile with "effective thickness" L, the intensity reflectivity coefficients for the extraordinary and ordinary waves will be given by

$$R_{||}\equiv R_{||}(n_{||},n_{\perp},n_{\rm iso},\theta_0,\delta,\xi_H,L) \tag{2}$$

and

$$R_{\perp}\equiv R_{\perp}(n_{\perp},n_{\rm iso},\delta,L)\ , \tag{3}$$

where $n_{||}$ and $n_{\perp}$ are the extraordinary and ordinary indices of the nematic LC at the clearing temperature T_c, respectively, $n_{\rm iso}$ is the refractive index of the isotropic phase at $T=T_c$, and δ is the incidence angle. In general, the theoretical values of $R_{||}$ and $R_{\perp}$ cannot be given in analytic form, but can be deduced by numerical integration of Maxwell equations according to the procedure proposed by Berreman.[25] In our experiments the magnetic coherence length ξ_H is always greater than 2 μm; then we can easily verify that the distortion of the director field due to the magnetic field gives a negligible contribution ($\sim 0.1\%$) to the reflectivity coefficient $R_{||}$. Therefore this contribution will be always disregarded in our analysis. Furthermore, the effective thickness L of the interface is much smaller than the wavelength λ of the incident laser beam. In these conditions, the reflectivity coefficients $R_{||}$ and $R_{\perp}$, at normal incidence, can be expressed via the simple analytic form[26]

$$R_J\simeq\left[\frac{1}{n_J+n_{\rm iso}}\int_{-\infty}^{+\infty}\frac{\partial n_j(z)}{\partial z}\exp[-2ik(z)z]dz\right]^2\ , \tag{4}$$

where $k(z)=2\pi n_J(z)/\lambda$, $j=1,2$ corresponds to $\perp$ or $||$, respectively.

B. Interfacial thickness

In order to calculate R_J we must assume a well-defined expression for the dependence of the refractive indices $n_{\perp}$ and $n_{||}$ on the z vertical coordinate near the interface. As concerns the contribution of the intrinsic diffuse profile of the interface we assume

$$n_J(z)=\frac{1}{2}\left[n_J+n_{\rm iso}+(n_{\rm iso}-n_J)\tanh\left[\frac{2z}{L_0}\right]\right]\ , \tag{5}$$

where n_J and $n_{\rm iso}$ represent the bulk refractive indices. This functional dependence will be justified in Sec. V in terms of the Landau–de Gennes theory[21] of the nematic-isotropic interface. By substituting Eq. (5) into Eq. (4) and by using the Born approximation [$k(z)=k=$const], one obtains[26]

$$R_J=R_{0J}\left[\frac{\pi\bar{k}L_0}{2\sinh\left[\frac{\pi\bar{k}L_0}{2}\right]}\right]^2\ , \tag{6}$$

where $\bar{k}\equiv(\pi/\lambda)(n_J+n_{\rm iso})=2\pi/\bar{\lambda}$ represents the average wave vector across the interfacial transition layer and R_{0J} represents the theoretical reflectivity coefficient for a sharp interface.

Thermal fluctuations of the nematic-isotropic interface give two different contributions to the intensity of the measured reflected light.[20]

(1) Small-wavelength capillary waves ($\lambda_c<\bar{\lambda}$) simulate an "apparent" diffuse profile of the interface which reduces the intensity of the reflected light, according to Eq. (4).

(2) High-wavelength capillary waves ($\lambda_c>\bar{\lambda}$) scatter the reflected light so to give a further reduction of the measured reflected intensity. The influence of this latter effect on the measured value of the reflectivity coefficients depends on the acceptance angle of the experimental optical apparatus. Both these contributions have been discussed in detail by Meunier and Langevin.[20] In the case of a sharp interface, they showed that the apparent reflectivity coefficient due to these contributions can be expressed as

$$R_J=R_{0J}\exp(-4\bar{k}^2L_T^2)\ , \tag{7}$$

where R_{0J} and $\bar{k}$ have been already defined and L_T is related to the mean square displacement due to capillary waves and is given by

$$L_T^2\equiv\frac{k_BT}{4\pi\gamma_{\rm eq}}\ln\left[\frac{q_{\rm max}^2l_c^2+1}{\bar{k}^2\sin^2\alpha l_c^2+1}\right]\ , \tag{8}$$

where k_B is the Boltzmann constant, $\gamma_{\rm eq}$ is the interfacial surface tension, $l_c=\gamma_{\rm eq}/\Delta eg$ is the capillary thickness, Δe is the density difference between the anisotropic and the isotropic phase, $q_{\rm max}$ is the largest wave vector of the fluctuations ($q_{\rm max}\sim\pi/L$), and α is the acceptance angle of the experimental apparatus. This angle is related to the diameter of the pinhole (D in Fig. 5) which selects the reflected light beam (in our measurements $\alpha=0.005$ rad). Notice that the value of $q_{\rm max}$ is not well defined; however, the logarithmic dependence of Eq. (8) ensures L_T is poorly dependent on the exact value of $q_{\rm max}$. In our case $q_{\rm max}^2l_c^2\gg1$ and $\bar{k}^2\sin^2\alpha\, l_c^2\gg1$ so that Eq. (8) can be approximated by

$$L_T^2\simeq\frac{k_BT}{2\pi\gamma_{\rm eq}}\ln\left[\frac{\lambda}{(n_J+n_{\rm iso})\alpha L}\right]\ . \tag{9}$$

Finally, one could expect also a reduction of the intensity of the reflected light due to fluctuations of the director orientation close to the interface. However, this latter effect is negligible in the present experiment. If the interface is not sharp but has a diffuse profile one has to take

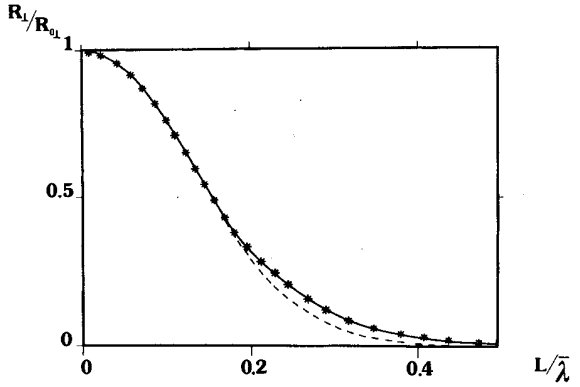

FIG. 3. Reflectivity coefficient for the TE mode as a function of the ratio of interfacial thickness L to the average wavelength $\bar{\lambda}$ of the electromagnetic wave. $\bar{\lambda}$ is defined by $\bar{\lambda}=2\lambda/(n_\perp+n_{\rm iso})$; where $n_{\rm iso}$ (1.56) and $n_\perp$ (1.53) are the refractive indices of the isotropic and anisotropic phase, respectively. The reflectivity coefficient is divided by the theoretical one ($R_{0\perp}$) corresponding to a sharp interface ($L=0$). Dashed curve corresponds to the Gaussian dependence given by Eq. (11) (for $L_T=0$). Solid line represents the dependence given by Eq. (6). Points correspond to the exact behavior obtained by numerical integration of Maxwell equations. Reflectivity coefficients are calculated for the experimental incidence angle $\delta=0.9°$.

account for both the previous contributions ($L_0\neq 0$, $L_T\neq 0$). In this case we cannot obtain an analytical expression for the reflectivity coefficients except in the case where the intrinsic diffuse profile goes as an error function, i.e.,

$$n_J(z)=\frac{1}{2}\left[n_J+n_{\rm iso}+\frac{2}{\pi}(n_{\rm iso}-n_J)\int_0^{2\sqrt{6}z/\pi L_0}dt\,\exp(-t^2)\right]. \tag{10}$$

If $L_0, L_T \ll \bar{\lambda}/2\pi$ we can easily show that Eqs. (10) and (5) give almost identical reflectivity coefficients (see Fig. 3). Therefore we are justified in using Eq. (10) in place of Eq. (5). In this case the effective reflectivity coefficient due to both the intrinsic and the thermal thickness can be obtained in the simple analytical form:[20]

$$R_J=R_{0J}\exp\left[-4\bar{k}^2\left[L_T^2+\frac{\pi^2}{48}L_0^2\right]\right]$$
$$=R_{0J}\exp\left[-\frac{\pi^2\bar{k}^2L^2}{12}\right] \tag{11}$$

and thus

$$L_0=\left[L^2-\frac{48}{\pi^2}L_T^2\right]^{1/2}. \tag{11'}$$

Figure 3 shows the dependence of the reflectivity coefficients ratio R_J/R_{0J} on $L_0/\bar{\lambda}$ when L_T is assumed to be zero. The solid line corresponds to the behavior given by Eq. (6), while the dashed line corresponds to the behavior given by Eq. (11) for $L_T=0$. Points represent the exact reflectivity coefficient as calculated by using the numerical procedure proposed by Berreman[25] and the interfacial profile of Eq. (5). Let us notice that, for small values of L_0, both Eq. (6) and Eq. (11) well approximate the exact behavior. Therefore by measuring the orthogonal reflectivity coefficient $R_\perp$ and by calculating the theoretical reflectivity coefficient for a sharp interface one can obtain from Eq. (11) the effective thickness L. The intrinsic thickness L_0 can be calculated, in turn, by using Eqs. (9) and (11'). Finally, the coherence length ξ of the order-parameter fluctuations will be given by

$$\xi=\frac{L_0}{4}=\frac{1}{4}\left[L^2-\frac{48}{\pi^2}L_T^2\right]^{1/2}. \tag{12}$$

C. Surface polar angle and anchoring energy

The easy surface polar angle θ_t of the director is obtained by measuring the ratio of the parallel to the orthogonal reflectivity coefficient. Figure 4 shows the theoretical dependence of this ratio on the surface polar angle θ_0 for some values of the ratio $L/\bar{\lambda}$. Note that $R_\parallel/R_\perp$ is poorly dependent on the thickness of the interface. The dependence of $R_\parallel/R_\perp$ on θ_0 is not monotonic, thus two different values of θ_0 can correspond to the same value of $R_\parallel/R_\perp$ (for example, $\theta_0=\theta_1$ and $\theta_0=\theta_2$ in Fig. 4). In order to remove the uncertainty between these two possible values one can increase the intensity of the applied magnetic field and measure the corresponding variation of the ratio $R_\parallel/R_\perp$. According to the elastic theory of LC, the increase of the magnetic field induces a corresponding increase of the surface polar angle θ_0; therefore $R_\parallel/R_\perp$ decreases if $\theta_0=\theta_1$ while it increases if $\theta_0=\theta_2$. The surface

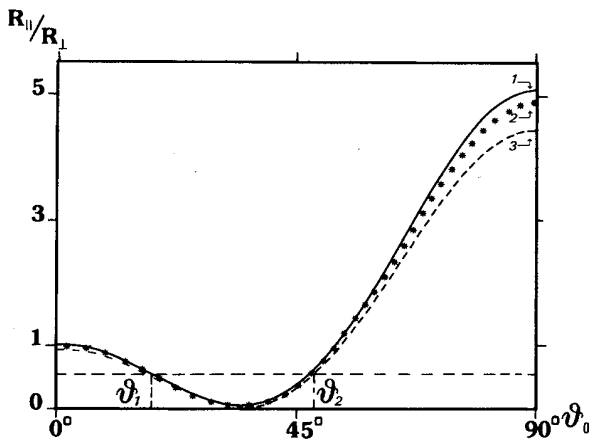

FIG. 4. Ratio of the reflectivity coefficients $R_\parallel$ to $R_\perp$ vs the polar angle θ_0 of the director at the interface. Curves denoted with 1, 2, and 3 correspond, respectively, to the following values of the ratio between the interfacial thickness and the wavelength $\bar{\lambda}$: $L/\bar{\lambda}=0$, $L/\bar{\lambda}=0.15$, and $L/\bar{\lambda}=0.3$. θ_1 and θ_2 indicate two different polar angles in correspondence of which the ratio $R_\parallel/R_\perp$ assumes the same value (curve 1). Both the reflectivity coefficients $R_\parallel$ and $R_\perp$ are calculated for the experimental incidence angle $\delta=0.9°$ and for $n_\perp=1.5335$, $n_\parallel=1.635$, and $n_{\rm iso}=1.564$ (7CB). Analogous curves with different vertical scales are obtained by using the refractive indices of the other compounds.

polar angle θ_t in the absence of external torques is obtained by extrapolating the $\theta_0(H)$ values to $H=0$.

The experimental analysis proceeds in two successive steps: first, from the measured value of $R_\perp$ we deduce the effective thickness L, then from the value of the ratio $R_{||}/R_\perp$ we deduce $\theta_0=\theta(H)$.

III. EXPERIMENTAL APPARATUS

The nematic materials we use are commercial 5CB, 6CB, 7CB, and 8CB produced by British Drug House Chemicals, Limited (BDH). We have verified that all these samples showed the proper clearing temperatures reported in the literature.[27] The geometry of the experimental cell containing the nematic LC is shown schematically in the inset of Fig. 5. The sample is enclosed in a cylindrical glass cell 1.5 cm wide and 2 cm high bounded by two horizontal glass plates. These plates are in contact with two copper plates maintained at two different temperatures T_1 and T_2. The temperature T_1 of the bottom plate is lower than that of the upper plate so that a temperature gradient parallel to the gravity field is present and thus the upper LC is isotropic, while the lower is anisotropic. The interface between two phases lies at a given vertical position z_0 that can be modified by changing the temperatures T_1 and T_2 of the copper plates. A small hole (diameter 3 mm) is opened on the upper copper plate in order to allow an incident laser beam to pass through. The temperature of both plates is held fixed within ± 0.05 °C. A Plexiglas box ensures the thermal insulation of the lateral walls of the cell from outside. The sample lies between the polar expansions of an electromagnet which generates a magnetic field ranging from 0.2 to 7.6 kG.

The experimental apparatus used to measure the optical reflectivity coefficients at the nematic-isotropic interface is schematically shown in Fig. 5. The glass plate G splits the He-Ne laser beam ($\lambda=6328$ Å) into two beams. The one is collected by the photodiode PH_1 that measures its intensity I_0, the other is polarized at 45° with respect to the magnetic field by the polarizer P and impinges with an incidence angle of 0.9° on the nematic-isotropic interface. The reflected beam passes through a Wollaston prism which splits the optical beams polarized in the direction parallel or orthogonal to the magnetic field. The intensities $I_\perp$ and $I_{||}$ of these two beams are measured by the photodiodes PH_2 and PH_3, respectively. Two analog dividers allow us to obtain the ratios $I_\perp/I_0$ and $I_{||}/I_0$ with an accuracy better than 0.2%. In order to obtain the absolute value of the reflectivity coefficients $R_\perp$ and $R_{||}$ it is necessary to calibrate the response of the photodiodes and account for losses due to reflections of the laser beam from the surfaces of the upper glass plate and due to the light scattering from the upper isotropic phase of the LC. The procedures used to calibrate the experimental apparatus have been already described in a previous letter.[18] Here it will suffice to note that the losses due to the glass plate are $\sim 15\%$, while the losses due to the isotropic phase of the nematic LC are, for example, $\sim 5\%$ in 7CB when the temperature gradient is 10 °C/cm. The measured value of losses due to light scattering from the upper isotropic phase agrees satisfactorily with the experimental data of Ref. 28. The experimental accuracy depends greatly on the accuracy of the alignment of the optical axis of the Wollaston prism along the magnetic field. By using a proper procedure we are able to perform this alignment within $\pm 0.5°$.

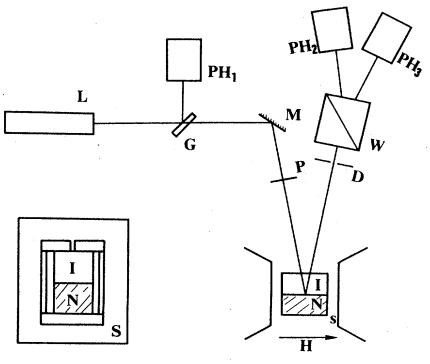

FIG. 5. Schematic view of the experimental apparatus. L, laser source; PH_1, PH_2, PH_3, photodiodes; G, glass plate; M, mirror; P, polarizer; D, diaphragm; W, Wollaston prism; S, sample; I, isotropic phase; N, nematic phase; H, magnetic field. The incidence angle of the laser beam is 0.9°. A schematic cross section of the thermostatic box is shown in the inset.

IV. EXPERIMENTAL RESULTS

Before performing the experiment we have verified that the measured values of $R_\perp$ and $R_{||}$ do not depend appreciably on the value of the temperature gradient across the nematic sample in the whole range from 1 to 15 °C/cm. Therefore we infer that thermal instabilities do not affect our measurements. Furthermore, we have verified that the experimental values of $R_\perp$ and $R_{||}$, corrected for losses, do not depend on the vertical position of the nematic-isotropic interface (within $\pm 5\%$). Finally, we have investigated the dependence of $R_\perp$ and $R_{||}$ on the x and y coordinates of the incidence point at the interface. The reflection angle of the laser beam showed some variations as the incidence point at the interface was shifted. This observation indicates that the nematic-isotropic interface is not a plane but exhibits some roughnesses due to the presence of surface disclinations analogous to those which have been predicted by de Gennes[29] some years ago. As a matter of fact, we find that the incident laser beam splits into two different reflected beams when it impinges on a well-defined line on the interface. This behavior indicates a discontinuous variation of shape of the interface. The geometry of these surface roughnesses is modified by the magnetic field. A detailed investigation of these textures has been given in a previous paper.[30] Here it suffices to note that the largest departure from planarity is always smaller than 1.5°. Furthermore, it is always possible to locate the incidence point in surface regions where deviations from planarity are smaller than $\pm 0.2°$. These deflections depend on the magnetic field intensity H. Therefore all variations of H must be followed by some slight adjustments of the positions of the diaphragm D and of the two photodiodes PH_2 and PH_3 in such a way to maximize the output signal.

Before discussing our experimental results we address briefly an important issue concerning the interfacial density profile. It is well known that the nematic-isotropic transition is first order and thus, one expects a small biphasic region when the temperature is close to the clearing temperature T_c. The temperature range ΔT of existence of this biphasic region should be an increasing function of the amount of impurities which are present in the sample. Our samples were obtained from British Drug House and showed a high purity. Therefore one could expect a very small, but nevertheless finite, value of ΔT. The biphasic region is characterized by the simultaneous occurrence of nematic and isotropic phase (bubbles) that could create enormous problems with the interpretation of our measurements. In our experiment the nematic sample is subjected to a vertical temperature gradient and thus, each point corresponds to a well-defined temperature $[T=T_1+(\partial T/\partial z)z]$. If ΔT is the existence range of the biphasic region one could expect a corresponding biphasic layer close to the interface having a thickness $L=\Delta T/(\partial T/\partial z)$. Therefore a change of the temperature gradient should induce a variation of the interfacial thickness and of the reflectivity coefficients. On the contrary, as previously discussed, we never do observe any variation of the reflectivity coefficients when the temperature gradient is increased by an order of magnitude. This observation seems to indicate that the biphasic bubble region does not influence our experimental measurements.

Furthermore, we point out that the interfacial thicknesses measured in the present experiment are of the order of 400Å and thus, in the biphasic layer, bubble diameters should be much smaller than 400 Å. These diameters seem to be unreasonably small since they should be associated to very high surface to bulk free energy ratios. In fact typical values of bubble diameters close to the nematic-isotropic phase transition are found in the range 10—100 μm.

Figure 6 shows the experimental values of the ratio $R_\perp/R_{0\perp}$ for 5CB, 6CB, 7CB, and 8CB as a function of the intensity of the applied magnetic field. Each experimental point corresponds to the average value of five different measurements. Reproducibility between different measurements for the same value of the magnetic field is better than $\pm 5\%$. The theoretical value of $R_{0\perp}$ (reflectivity coefficient for a sharp interface) is obtained by using the average value of the refractive indices measured by Dunmur *et al.*[31] and by Karat and Madhusudana[32] and extrapolated to the clearing temperature. These indices are given in Table I. The experimental values of Ref. 31 have been extrapolated to the wavelength $\lambda=6328$ Å by using the empirical relation given in the same reference. The estimated accuracy of these average values is $\Delta n=\pm 0.002$. Table I shows the average refractive indices $n_\perp$, $n_\parallel$, and $n_{\rm iso}$, together with other physical coefficients that will be used later. Notice that, if $H>2$ kG the experimental values of $R_\perp/R_{0\perp}$ are almost independent of

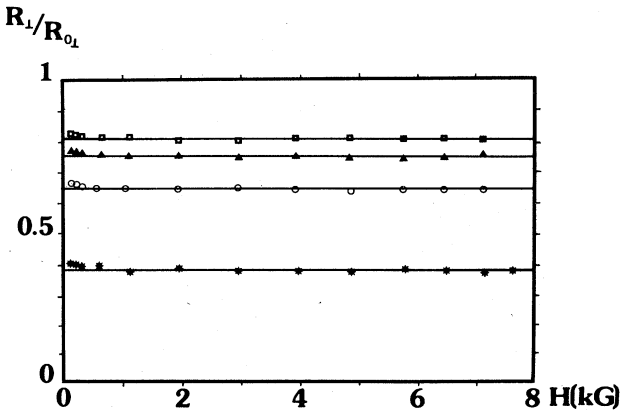

FIG. 6. Experimental orthogonal reflectivity coefficients as a function of the intensity H of the magnetic field for 5CB (▲), 6CB (*), 7CB (○), and 8CB (□). Experimental reflectivity coefficients are divided by the theoretical ones expected in the case of a sharp interface. Theoretical reflectivity coefficients have been calculated by using the average refractive indices given in Table I.

TABLE I. Some physical coefficients of cyanobiphenyls at the clearing temperature. $n_\parallel$, $n_\perp$, and $n_{\rm iso}$ are the average values of two independent measurements (Refs. 31 and 32) of the extraordinary, the ordinary, and the isotropic refractive indices. T_c is the clearing temperature; T^* and a are characteristic parameters of the Landau—de Gennes theory (Ref. 21). All these parameters have been obtained from Ref. 28. $\chi_a=\chi_\parallel-\chi_\perp$ is the anisotropy of the diamagnetic susceptibility (Ref. 33), while $\gamma_{\rm eq}$ is the surface tension of the nematic-isotropic interface (Ref. 23). K is the average value of the two elastic constants K_{11} and K_{33}. These elastic constants have been measured some years ago by Karat and Madhusudana (Refs. 32 and 47) but their results are shown to be incorrect (Ref. 48). Correct values of the elastic constants are given in Ref. 49.

Coefficient	5CB	6CB	7CB	8CB
$n_\perp$ (± 0.002)	1.5490	1.5480	1.5335	1.5336
$n_\parallel$ (± 0.002)	1.6516	1.6454	1.6350	1.6250
$n_{\rm iso}$ (± 0.002)	1.5792	1.5756	1.5640	1.5598
T_c (°C) (± 0.2)	34.3	30.1	42.6	40.2
T^* (°C) (± 0.2)	32.9	28.7	41.5	38.2
a (10^5 erg/cm^3°C) (± 1)	12	19	24	19
K (10^{-7} erg/cm) (± 0.3)	2.1	2.2	2.3	2.0
χ_a (10^{-7} emu) (± 0.005)	0.708	0.597	0.623	0.558
$\gamma_{\rm eq}$ (10^{-2} erg/cm^2)	1.49±0.6	0.71±0.4	1.82±0.7	0.95±0.4

the magnetic field, while they exhibit some residual dependence on H for $H<2$ kG (in particular in the case of 6CB). This latter dependence is probably due to the fact that low magnetic fields are not able to orient completely the director along the x axis in the horizontal plane. Therefore the experimental values of the reflectivity coefficients for $H<2$ kG are not very accurate. For this reason, the reflectivity coefficients in the absence of external torques are obtained by extrapolating to $H=0$ the experimental values in the large magnetic field region ($H>2$ kG). By substituting into Eq. (11) the extrapolated value of $R_\perp/R_{0\perp}$ we obtain the effective thickness L. The thermal thickness due to capillary waves at the interface can be calculated by substituting in Eq. (9) the known values of the interfacial surface tension γ_{eq} and of the effective thickness L. Finally, by using Eq. (11') one can estimate the intrinsic thickness L_0 of the interface. Unfortunately both the effective thickness L and the thermal thickness L_T are affected by a large uncertainty and thus, one cannot obtain a well-defined value of the intrinsic thickness but only a higher limit. Table II reports the measured values of the effective thickness L, the surface polar angle θ_t, and the anchoring energy coefficient W together with the estimated values of the thermal thickness L_T and the higher limits of the intrinsic thickness L_0 and of the coherence length (ξ_{expt}). ξ_{theor} corresponds to the theoretical value of the coherence length as given by the Landau–de Gennes theory [see Eq. (24)]. The experimental uncertainty of the effective thickness is mostly due to the uncertainty of the refractive indices of the nematic LC ($\Delta n\simeq\pm0.002$) and to the spurious effect of light scattering from the upper glass window of the cylindrical cell containing the nematic LC. Other minor error sources have been discussed in a previous paper.[18] The uncertainty of the estimated thermal thickness L_T is mostly due to the uncertainty of the surface tension γ_{eq}. We point out that the accuracy of the thickness measurements in the present experiment is very poor since $L/\bar{\lambda}\ll1$. Therefore we can only obtain here a rough estimate of the coherence length. The higher limits of ξ are consistent with the experimental values of ξ obtained by light scattering in MBBA [ξ(MBBA)$=115$ Å].

Note that, in principle, the order parameter S in the isotropic and anisotropic phase could increase when the magnetic field is switched on. This effect should be more relevant in the proximity of the interface where the local temperature is the clearing temperature T_c. As a consequence of this effect the refractive indices $n_\perp$, $n_{||}$, and n_{iso} would change. In particular the upper isotropic phase would become slightly birefringent and the ordinary and extraordinary indices would change according to

$$\frac{|\Delta n_\perp|}{n_{iso}-n_\perp}\simeq\frac{|\Delta n_{||}|}{n_{||}-n_{iso}}\simeq\frac{\Delta S(H)}{S_c}\ , \tag{13}$$

where $\Delta S(H)$ represents the variation of the order parameter due to the magnetic field. By using the Landau–de Gennes expansion of the free energy density[21] one can easily show that the variation of $n_\perp$, $n_{||}$, and n_{iso} induced by the magnetic field is

$$|\Delta n_\perp|\simeq\tfrac{1}{2}|\Delta n_{||}|\simeq|\Delta n_{iso}|\simeq\frac{(n_{iso}-n_\perp)\chi_\alpha H^2\sin^2\theta_t}{3a(T_c-T^*)}\ , \tag{14}$$

where χ_α is the anisotropy of the diamagnetic susceptivity and a and T^* are two characteristic coefficients of the Landau–de Gennes theory. By using the experimental values of χ_α measured by Sherrel and Crellin[33] and those of a and T^* measured by Coles and Stratielle[28] we obtain (for $H=10^4$ G and $\theta_t=90°$)

$$\Delta n<10^{-7}$$

which is a value far below our experimental sensitivity.

TABLE II. Experimental values of the easy director polar angle θ_t, the anchoring energy coefficient W, the effective thickness L [Eq. (11)], the intrinsic thickness L_0 [Eq. (11')], the thermal interfacial thickness L_T [Eq. (9)], and the coherence length ξ_{expt}. ξ_{theor} corresponds to the theoretical value of the coherence length as predicted by the Landau–de Gennes theory [Eq. (24)]. These parameters for 7CB were already published in Ref. 18. However, the anchoring energy coefficient reported here differs from the previous one since the latter was obtained by using the incorrect elastic constants given in Ref. 47 (see caption of Table I). Furthermore, a slight difference between the values reported here of θ_t and L for 7CB and the previous ones is due to the fact that in the previous paper we used the refractive indices given in Ref. 32, only.

Coefficient	5CB	6CB	7CB	8CB
θ_t (deg)	63.5±6	64.5±6	52.6±6	48.5±6
W (10^{-4} erg/cm^2 rad^2)	4.8±1.2	0.84±0.2	8.3±2.2	8.5±2.1
L (Å)	382 ±200	720 ±100	450 ±150	355 ±200
L_0 (Å)	<485	<700	<520	<380
L_T (Å)	180 ±50	245 ±100	160 ±50	225 ±80
ξ_{expt} (Å)	<120	<175	<130	<95
ξ_{theor} (Å)	87 ±50	56 ±40	85 ±50	22 ±18

Therefore this effect can be completely neglected in the present experiment.

Figure 7 shows the experimental values of the ratio $R_{\parallel}/R_{\perp}$ as a function of the magnetic field intensity. Also in this case the experimental values of $R_{\parallel}/R_{\perp}$, for $H<2$ kG, are affected by spurious effects due to the reorientation of the director in the horizontal plane. The case of 6CB is a pathological one, since a noticeable saturation effect is present in the high-field regime. This saturation indicates that the surface polar angle is close to 90°. In order to find the surface director polar angle θ_t we substitute the experimental values of $R_{\parallel}/R_{\perp}$ in Fig. 4. The experimental values of θ_0 as a function of the magnetic field are reported in Fig. 8.

In order to find the anchoring energy coefficient W we calculate the surface polar angle $\theta_0(H)$ by using the Frank-Eriksen theory[34] in the case of isotropic elastic constants ($K_{11}=K_{33}=K$) and by using Eq. (1) for the surface tension. If $\theta_0-\theta_t \ll 1$ one easily obtains

$$\theta_0=\theta_t+\frac{\sqrt{K\chi_a}\cos\theta_0 H}{2W}\ , \tag{15}$$

where K is the average elastic constant [$K=(K_{11}+K_{33})/2$] at the clearing temperature T_c, while χ_a is the magnetic susceptibility anisotropy. Experimental values for these constants are reported in Table I. To obtain Eq. (5) we have neglected the nonuniformity of the temperature in the sample. This approximation is well justified in our experiment since, for $H>2$ kG, the thickness of the distorted layer near the interface is lower than $h\sim 10\ \mu$m. In this case, the temperature variations across the distorted layer are lower than $\Delta T=\Delta T h/\Delta z\sim 10^{-2}$ °C. By comparing the experimental dependence of θ_0 on the magnetic field intensity with the theoretical one [Eq. (15)] we obtain the anchoring energy coefficient W. Continuous curves in Fig. 8 correspond to the best fit of Eq. (15) to the experimental points. Both the easy polar angle θ_t and the anchoring energy coefficient are obtained by the best fit (see Table II). Figures 9(a) and 9(b) show the easy polar angle and the anchoring energy coefficient versus the length of the alkylic chain.

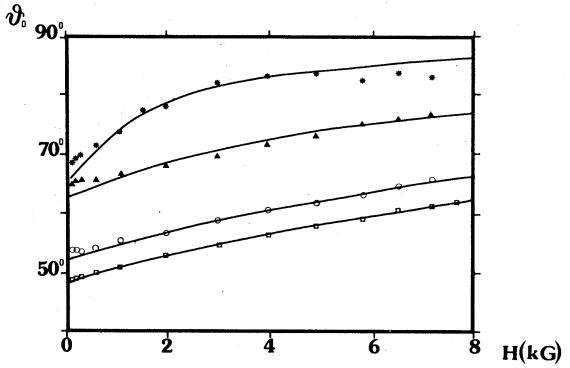

FIG. 8. Polar angle of the director at the free surface of 5CB (▲), 6CB (*), 7CB (○), and 8CB (□), vs the magnetic field. The values of θ_0 have been calculated by using the experimental values of $R_{\parallel}/R_{\perp}$ and of the interfacial thickness L.

All the measured anchoring energy coefficients (Table III) are smaller than 10^{-3} erg/cm^2 rad^2 and exhibit a minimum value ($\sim 0.8\times 10^{-4}$) in 6CB. Note that all these coefficients are much lower than the corresponding interfacial surface tensions (see Table II). Therefore we infer that the anisotropic contribution to the surface excess of free energy is a small fraction of the total one.

It can be, now, interesting to compare the anchoring energy at the nematic-isotropic interface with that measured at solid-nematic interfaces. Many authors measured anchoring energy coefficients for different substrates and surfactants by using different experimental techniques.[1,35–42] They found energy values spaced between 10^{-4} and 10^{-2} erg/cm^2 rad^2. Our experimental results are comparable with the weakest anchoring energies measured by Porte[35] on a glass substrate covered with a monomolecular film of aliphatic monoammines and by Ryschenckov[36] on a glass substrate covered with a film of car-

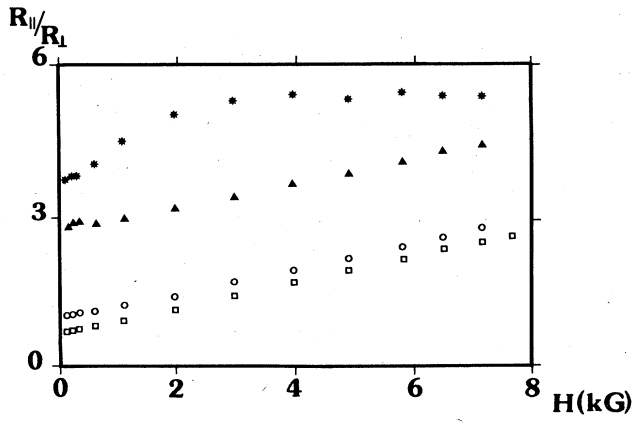

FIG. 7. Experimental values of the ratio $R_{\parallel}/R_{\perp}$ as a function of the intensity H of the magnetic field for 5CB (▲), 6CB (*), 7CB (○), and 8CB (□).

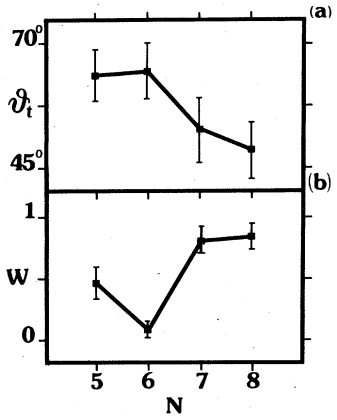

FIG. 9. (a) Polar angle of the director vs the number N of carbon atoms of the alkylic chain. (b) Anchoring energy coefficient vs N. The unities of the vertical axis (W) are 10^{-3} erg/cm^2 rad^2.

TABLE III. Experimental values of the phenomenological coefficients γ_0, γ_Q, and γ_P of the Parsons theory of the interfacial tension (Ref. 4).

Coefficient	5CB	6CB	7CB	8CB
γ_0 (10^{-2} erg/cm^2)	1.5 ±0.6	0.71±0.4	1.82±0.7	1.02±0.4
γ_P (10^{-4} erg/cm^2)	5.31±2	0.89±0.4	16.0 ±7	20.1 ±8
γ_Q (10^{-4} erg/cm^2)	11.9 ±5	2.06±0.8	26.3 ±10	30.4 ±10

bon black from overheated cellulose.

Finally, let us compare the anchoring energy coefficients of nematic-isotropic interfaces with those of nematic-vapor interfaces (free surfaces). Few experimental data on these latter coefficients are available in the literature.[41–43] Proust *et al.* studied asymmetrical thin films of 5CB obtained by spreading a small nematic drop on a water surface.[41] The easy director orientation at the water-nematic interface is found to be parallel to the layer, while it is orthogonal at the upper free surface. Therefore the director orientation in the nematic layer is distorted. When the layer thickness is below some critical value, the director orientation becomes parallel to both surfaces in the whole layer. This critical thickness allows them to measure the free-energy difference $\gamma_{\parallel}-\gamma_{\perp}$ between parallel and orthogonal orientation at the free surface, respectively. By assuming that the anchoring energy at the free surface can be expressed as $W_a = W\sin^2\theta_0$, Proust *et al.* obtained the anchoring energy coefficient $W=\gamma_{\parallel}-\gamma_{\perp}\sim 4\times 10^{-3}$ erg/cm^2 rad^2. Recent measurements we have performed at the free surface of some cyanobiphenyls,[43] by using the same experimental technique discussed in this paper, allow us to obtain $W(5\text{CB})>0.6\times 10^{-1}$ erg/cm^2 rad^2, which is a value much higher than the previous one. According to Proust *et al.*[41] this experimental result seems to indicate that the simple expressions $W_a = W\sin^2\theta_0$ is not well suited to a free surface. Similar high values of the anchoring energy coefficient have been measured at the free surface of MBBA.[42] Therefore, the anchoring energy coefficients at the nematic-isotropic interface are much smaller than the ones at the free nematic interface.

In order to evidence possible hysteresis effects due, for example, to the presence of a double-well shape of the surface tension[44] (see Fig. 1), we have increased the temperature of the bottom plate above the clearing temperature T_c in such a way that the whole LC was in the isotropic phase. Then, we have applied a 7.6-kG magnetic field and we have restored the original temperature gradient. The reflectivity coefficients measured in these conditions coincided, within the experimental reproducibility ($\sim 5\%$), with the previous ones. Therefore no hysteresis is found in our experiment.

V. DISCUSSION

A. Intrinsic thickness of the interface

The intrinsic thickness of the interface is related to the spatial variation of the scalar order parameter $S(z)$ across the interface. In fact this order parameter has to change from the finite value S_c in the anisotropic phase, close to the interface, to the zero value in the isotropic phase. The Euler-Lagrange equation which establishes the space dependence of the order parameter close to the interface has been obtained by de Gennes some years ago.[21] Here we review the main results of the de Gennes theory and we calculate explicitly the z dependence of the order parameter. The starting point of the de Gennes theory is the well-known Landau–de Gennes expansion of the Helmholtz free energy per unit volume:

$$F\equiv F_0+\frac{A}{2}S^2-\frac{B}{3}S^3+\frac{C}{4}S^4+\frac{A}{2}\xi^2\left[\frac{dS}{dz}\right]^2, \tag{16}$$

where F_0 is the isotropic free energy; A, B, and C are phenomenological coefficients; and ξ is the coherence length of the order-parameter fluctuations which depends on the θ_0 polar angle. The coefficients in Eq. (16) have been defined in a slightly different way with respect to the ones of Ref. 21. Equation (16) has been written in the hypothesis that the director polar angle does not change across the interface. Since the thickness of the interface is very small (~ 500 Å), we can neglect completely the temperature variations across the interface and thus, we can consider $T=T_c=\text{const}$. In correspondence with this temperature value, F is represented by a double well having two minima $F_1=F_2=F_0$ at $S=0$ and $S=S_c=2B/3C$, while the coefficients A, B, and C must satisfy the condition

$$\frac{B^2}{AC}=\frac{9}{2} \tag{17}$$

and A is given by

$$A\equiv a(T_c-T^*), \tag{18}$$

where a is a constant positive coefficient and T^* is a critical temperature close to T_c ($T_c-T^*\sim 1\,^\circ$C). The surface excess of Helmholtz free energy per unit area is

$$\gamma\equiv\int_{-\infty}^{+\infty}(F-F_0)dz\ . \tag{19}$$

The actual profile of the order parameter $S(z)$ can be obtained by minimizing Eq. (19) with respect to variations of S. One obtains

$$\frac{d^2S}{dz^2}=\frac{1}{\xi^2}\left[S-3\frac{S^2}{S_c}+2\frac{S^3}{S_c^2}\right], \tag{20}$$

with the following boundary conditions:

$$S\to 0 \quad \text{for } z\to+\infty \tag{21}$$

and

$$S \to S_c \quad \text{for } z \to -\infty \ . \tag{21'}$$

The order-parameter profile across the interface is, then, given by

$$S(z)=\frac{S_c}{2}\left[1+\tanh\left[-\frac{z}{2\xi}\right]\right], \tag{22}$$

which is just of the same kind as Eq. (5). By comparing Eq. (22) with Eq. (5) one obtains

$$\xi=\frac{L_0}{4} \ . \tag{23}$$

By substituting Eq. (22) into Eq. (19) one obtains the following expression for the surface tension:[45]

$$\gamma_{\rm eq}=\frac{A\xi S_c^2}{6} \ . \tag{24}$$

Equation (24) allows us to obtain the coherence length ξ from a measurement of the surface tension $\gamma_{\rm eq}$. By using the values of $\gamma_{\rm eq}$ given in Ref. (23) and the values of a and S_c given in Ref. (28) we obtain the theoretical coherence lengths $\xi_{\rm theor}$ shown in Table II. We notice that the accuracy of $\xi_{\rm theor}$ is very poor due to the uncertainty of the experimental values of $\gamma_{\rm eq}$, A, and S_c. Comparison between the values of ξ measured here and the theoretical ones indicates that Eq. (24) furnishes the correct order of magnitude of the interfacial thickness. Unfortunately, the high experimental uncertainty of the ξ measurement does not allow us to obtain a clear comparison of experiment with theory.

Let us notice, however, that Eqs. (22) and (24) have been obtained by using the power expansion of Eq. (16) which holds, in principle, only for $S \ll 1$. This is not the case of the order parameter in the anisotropic phase and therefore, one expects that Eqs. (22) and (24) furnish only the qualitative behavior of the interface. Furthermore, many authors[3–5] showed that the presence of an interface breaks the original symmetry of the system and thus it should be necessary to add a new term in Eq. (16) which is proportional to the local order parameter. This latter term can have important consequences regarding the interfacial properties. Finally, we remark that the Landau–de Gennes theory, in the present form, predicts only two possible easy directions at the nematic-isotropic interface: $\theta_t=0°$ or 90°. This prediction is not satisfied in the nematic samples considered here. A question arises as to whether the tilted alignment could be explained by generalizing Eq. (16) to account for possible orientational distortions across the interface.[21]

B. Surface director orientation and anchoring energy

In recent years many theories[2–4,8,21] have been proposed to explain the easy orientation of the director at the interface. However, most of these theories predict only two possible values of the easy tilt angle ($\theta_t=0°$, $\theta_t=\pi/2$). Among all these theories only the Mada theory[3] and the Parsons theory[4] are able to explain the tilted alignment that has been observed at the free surface and at the nematic-isotropic interface of some nematic LC. However, the authors of Ref. 19 recently showed that some results of the Mada theory are incorrect. In the following we will consider the Parsons theory. According to this theory the tilted alignment is interpreted as being due to the competition between two different mechanisms: the orienting effect of van der Waals forces of quadrupolar symmetry which tend to align the molecules parallel to the interface and the polar orienting effect due to the presence of a density gradient close to the interface and tending to orient the molecules orthogonal to the interface. This latter effect can occur if the two ends of the molecules are not equivalent. The corresponding expression of the interfacial free energy is

$$\gamma=\gamma_0+\tfrac{1}{2}\gamma_Q(\vec{n}\cdot\vec{k})^2-\gamma_P\vec{n}\cdot\vec{k} \ , \tag{25}$$

where γ_0, γ_Q, and γ_P are positive phenomenological coefficients and $\vec{n}$ and $\vec{k}$ are the director and the versor of the vertical axis, respectively. γ_Q accounts for the effect of quadrupolar forces, while γ_P accounts for the polar effect. Minimization of Eq. (25) with respect to $\vec{n}\cdot\vec{k}=\cos\theta_0$ gives

$$\theta_t=\begin{cases}\arccos\left[\dfrac{\gamma_P}{\gamma_Q}\right] & \text{for } \gamma_P<\gamma_Q \\ 0 \ \text{ for } \gamma_P\geq\gamma_Q \ .\end{cases} \tag{26}$$

In our case $\theta_t\neq 0$ and thus $\gamma_P<\gamma_Q$. Close to the angle $\theta_0=\theta_t$ the surface free energy can be expanded in a power series of $(\theta_0-\theta_t)$ as

$$\gamma=\gamma_0-\frac{1}{2}\frac{\gamma_P^2}{\gamma_Q}+\frac{1}{2}\left[\gamma_Q-\frac{\gamma_P^2}{\gamma_Q}\right](\theta_0-\theta_t)^2+\cdots \tag{27}$$

(where the ellipsis represents unspecified higher-order terms) by comparing Eq. (27) with Eq. (1) one obtains

$$\begin{aligned}\gamma_{\rm eq}&=\gamma_0-\frac{1}{2}\frac{\gamma_P^2}{\gamma_Q} \ , \\ W&=\frac{1}{2}\left[\gamma_Q-\frac{\gamma_P^2}{\gamma_Q}\right] \ .\end{aligned} \tag{28}$$

Therefore, from the measured values of θ_t, W, and $\gamma_{\rm eq}$ one can obtain all the phenomenological coefficients of this theory. The values of $\gamma_{\rm eq}$ have been recently measured by us[23] by using the sessile drop method. Table III shows the calculated values of γ_0, γ_Q, and γ_P for 5CB, 6CB, 7CB, and 8CB.

A question arises as to how the phenomenological coefficients γ_0, γ_Q, and γ_P are related to the microscopic molecular parameters characterizing the nematic samples studied here. Unfortunately, so far no microscopic calculations of these coefficients have been performed.

VI. CONCLUDING REMARKS

In this paper we report the first experimental measurements of the effective thickness of the polar angle of the director and of the anchoring energy at the nematic-isotropic interface of 5CB, 6CB, 7CB, and 8CB. The measured thickness comes, in principle, from the superpo-

sition of two different contributions: intrinsic diffuse profile of the interface and apparent diffuse profile due to thermal fluctuations. The thermal contribution is evaluated by using the known values of the surface tension γ_{eq}, while a higher limit for the intrinsic thickness is obtained by using the experimental values of the effective thickness. Unfortunately the accuracy of the thickness measurements is very poor since the wavelength λ of the laser beam is much greater than the thickness. Therefore, no definitive conclusions regarding the validity of the Landau—de Gennes approach can be obtained. New measurements performed at smaller wavelengths should be required. As concerns the surface polar angle θ_t and the anchoring energy, we have found that the director at the nematic-isotropic interface of all these samples is tilted with respect to the vertical axis. The measured anchoring energies are found to be very small, $< 10^{-3}$ erg/cm^2 rad^2, for all these samples and they exhibit their minimum value in 6CB. From these measurements we infer that the orientational contribution to the surface tension is of the order of 10%.

ACKNOWLEDGMENTS

This research was supported in part by Ministeso della Pubblica Istruziome (Italy) and in part by Consiglio Nazionale delle Ricerche (Italy).

*Also at Gruppo Nazionale di Struttura della Materia del Consiglio Nazionale delle Ricerche, I-56100 Pisa, Italy.
[1]J. Cognard, Mol. Cryst. Liq. Cryst. Suppl. 1, 1 (1982).
[2]J. D. Parsons, Mol. Cryst. Liq. Cryst. **31**, 79 (1975).
[3]H. Mada, Mol. Cryst. Liq. Cryst. **51**, 43 (1979); **53**, 127 (1979).
[4]J. D. Parsons, Phys. Rev. Lett. **41**, 877 (1978).
[5]C. A. Croxton, Mol. Cryst. Liq. Cryst. **66**, 223 (1981).
[6]C. A. Croxton, Mol. Cryst. Liq. Cryst. **59**, 219 (1980).
[7]C. A. Croxton and S. Chandrasekar, Proceedings of the First International Conference on Liquid Crystals, Bangalore, 1973 (unpublished).
[8]J. D. Parsons, J. Phys. (Paris) **37**, 1187 (1976).
[9]J. Murakami, J. Phys. Soc. Jpn. **42**, 210 (1977).
[10]J. Bernasconi, S. Strassler, and H. R. Zeller, Phys. Rev. A **22**, 276 (1979).
[11]C. Rosenblatt and D. Ronis, Phys. Rev. A **23**, 305 (1981).
[12]M. A. Bouchiat and D. Langevin-Cruchon, Phys. Lett. **34**, 331 (1971).
[13]J. E. Proust and L. Ter-Minassian-Saraga, Colloid Polym. Sci. **259**, 1133 (1977).
[14]P. Chiarelli, S. Faetti, and L. Fronzoni, J. Phys. (Paris) **44**, 1061 (1983); S. Faetti and L. Fronzoni, Solid State Commun. **25**, 1087 (1978).
[15]D. Langevin-Cruchon and M. A. Bouchiat, Mol. Cryst. Liq. Cryst. **22**, 317 (1973).
[16]D. Langevin-Cruchon and M. A. Bouchiat, C. R. Acad. Sci. (Paris) **277**, 731 (1973).
[17]R. Vilanove, E. Guyon, C. Mitescu, and P. Pieransky, J. Phys. (Paris) **35**, 153 (1974).
[18]S. Faetti and V. Palleschi, J. Phys. (Paris) Lett. **45**, L313 (1984).
[19]G. Barbero, R. Bartolino, and M. Meuti, J. Phys. (Paris) Lett. (to be published).
[20]J. Meunier and D. Langevin-Cruchon, J. Phys. (Paris) Lett. **43**, L185 (1982).
[21]P. G. de Gennes, Mol. Cryst. Liq. Cryst. **12**, 193 (1971).
[22]E. Gulari and B. Chu, J. Chem. Phys. **62**, 798 (1975).
[23]S. Faetti and V. Palleschi, J. Chem. Phys. (to be published).
[24]D. A. Dunmur and W. H. Miller, J. Phys. (Paris) Colloq. **40**, C3-141 (1979).
[25]D. W. Berremann, J. Opt. Soc. Am. **62**, 502 (1972).
[26]J. S. Huang and W. W. Webb, J. Chem. Phys. **50**, 3677 (1969).
[27]G. W.Gray, J. Phys. (Paris) Colloq. **36**, C1-337 (1975).
[28]H. J. Coles and C. Stratielle, Mol. Cryst. Liq. Cryst. **55**, 273 (1979).
[29]P. G. de Gennes, Solid State Commun. **8**, 213 (1970).
[30]S. Faetti and V. Palleschi (unpublished).
[31]D. A. Dunmur, M. R. Manterfield, W. H. Miller, and J. K. Dunheavy, Mol. Cryst. Liq. Cryst. **45**, 127 (1978).
[32]P. P. Karat and N. V. Madhusudana, Mol. Cryst. Liq. Cryst. **36**, 51 (1976).
[33]P. L. Sherrel and D. A. Crellin, J. Phys. (Paris) Colloq. **40**, C3-211 (1979).
[34]P. G. de Gennes, *The Physics of Liquid Crystals* (Clarendon, Oxford, 1979).
[35]G. Porte, J. Phys. (Paris) **37**, 1245 (1976).
[36]G. Ryschenkov, Third Cycle Thesis, Orsay, 1975.
[37]D. Riviere, Y. Levy, and E. Guyon, J. Phys. (Paris) Lett. **40**, L215 (1979).
[38]J. Sicart, J. Phys. (Paris) Lett. **37**, L25 (1976).
[39]S. Naemura, Mol. Cryst. Liq. Cryst. **68**, 183 (1981).
[40]K. H. Young and C. Rosenblatt, Appl. Phys. Lett. **43**, 62 (1983).
[41]J. E. Proust, E. Perez, and L. Ter-Minassian-Saraga, Colloid Polym. Sci. **254**, 672 (1976).
[42]P. Chiarelli, S. Faetti, and L. Fronzoni, Phys. Lett. **101A**, 31 (1984).
[43]V. Palleschi, Tesi di Laurea, Università di Pisa, 1984.
[44]R. G. Horn, J. N. Israelachvili, and E. Perez, J. Phys. (Paris) **42**, 39 (1981).
[45]D. Langevin-Cruchon, These du doctorat, Paris, 1974.
[46]L. Senbetu and C. W. Woo, Mol. Cryst. Liq. Cryst. **84**, 101 (1982).
[47]P. P. Karat and N. V. Madhusudana, Mol. Cryst. Liq. Cryst. **40**, 239 (1977).
[48]J. D. Bunning, T. E. Faber, and P. L. Sherrel, J. Phys. (Paris) **42**, 1175 (1981).
[49]N. V. Madhusudana and R. Pratibha, Mol. Cryst. Liq. Cryst. **89**, 249 (1982).